5-2019

The 3D scaffold design of de novo anterior cruciate ligament graft

Dominique Angibeau

The 3D scaffold design of de novo anterior cruciate ligament graft

by

Dominique Angibeau

Undergraduate honors thesis under the direction of

Dr. Mandi Lopez

Department of Biological Engineering

Submitted to the LSU Roger Hadfield Ogden Honors College in partial fulfillment of the Upper Division Honors Program.

May, 2019

Louisiana State University
& Agricultural and Mechanical College
Baton Rouge, Louisiana

Abstract

Anterior cruciate ligament (ACL) injuries are the most common knee injuries in humans and canines. Reconstruction of ACL is performed with autologous or allogenic grafts, which are limited by donor site morbidity and scarcity. De novo generation of ACL using scaffolds to provide mechanical strength and cells to render viable factors is an appealing alternative to circumvent these limitations. We hypothesized truss-like structure improves mechanical strength of scaffolds.

Using triangle mesh pattern as texture, two scaffolds (oval tubes with or without 30° twist), a sheet and a mold for sheet were designed with Fusion 360. Tension force of 400 N on both ends of scaffolds was applied under computational simulation. Four scaffold materials were selected for simulation: polylactic-acid (PLA), polyglycolic-acid (PGA), polydioxanone (PDS) and collagen. Outcome parameters included safety factor, stress, displacement and strain.

PDS, PGA, and PLA displayed a maximum safety factor of 15 while that of collagen was 0.01818. As for stress, PDS displayed the highest Von Mises stress of 53.5 MPa, compared to the maximum value of 52.48 MPa for PGA, 51.66 MPa for PLA, and 51.44 MPa for collagen. The smallest displacement of the materials was 0.3056 mm which was PGA, while PDS had 0.7618 mm displacement, PLA with a 28.02 mm displacement, and collagen with a 109042 mm displacement. For strain, PDS with 0.02457, PGA with 0.00936, PLA with 0.8171, and collagen with 3132.

From the static stress analysis, the polymers, specifically, PGA, is seen as the most mechanically fit material for the scaffold design.

Acknowledgements

I would first like to thank Dr. Lopez for her guidance and support throughout my research. I am thankful for the challenge and inspiration which she has provided me throughout this research. I would also like to thank Takashi Taguchi for taking his time to teach and assist me in my research and writing. I greatly appreciate the Laboratory of Equine and Comparative Orthopedic Research for their encouragement and resources which they have provided me.

I would like to thank the Honors College and the Biological and Agricultural Engineering department for fostering education at Louisiana State University. I thankful for the education experience they have provided for me which helped me complete this process. In addition, the college and department have served as a great support system throughout my undergraduate career.

Lastly, I would like to thank my family. They were the ones who first encouraged me to apply for the Honors College and encouraged me to strive for College Honors. I am thankful for their everlasting support which motivates me every day.

Table of Contents

The 3D scaffold design of de novo anterior cruciate ligament graft

1. Introduction

The anterior cruciate ligament (ACL) is the most common knee injury seen in humans and canines. Due to the complexity of the ligament and the location, current treatments have not been able to restore the full use of the ligament. Today, tissue engineering is being studied with the intention to combat ACL injuries. The use of scaffolds composed of biomaterials show promise in maintaining the mechanical strength and fostering tissue growth. The design and material selection are crucial in order to reach full mechanical strength, biocompatibility, biodegradability, and tissue growth. By using 3D design programs, designs are able to be made with precision. In addition, the use of 3D printing allows for the use innovative technology that aids with accuracy and precision of creative objects. With the use of Fusion 360, design of a scaffold, which can sustain mechanical properties of the ACL, printed by using a 3D printer, and house the growth of cells.

1.1. ACL

Knee joint is comprised of 3 bones, tibia, femur and patella, and ligaments stabilizing bones, all of which are encapsulated by synovium. Ligaments of knee include patellar ligament anterior to knee, collateral ligaments on both medial and lateral sides of the knee, and anterior/posterior cruciate ligaments. Among these, ACL attached to the lateral condyle of the femur and the anterior ridge tibia incurs most injuries [1, 2]. ACL is made up of two bands, the anteromedial band and posterolateral band [3]. Its function is to limit hyperextension and internal rotation of tibia [4]. Whenever the knee moves from extension to flexion, the length of the ACL changes by elongating [2, 4]. Similar to other ligaments in the body, it has Type I collagen as a main component [4]. It is made up of three intertwined chains of amino acids, two alpha 1 chains and

one alpha 2 chains, which are linked together [4]. The strength of the collagen originated from parallel alignment of fibers cross-linked to each other. ACL injuries are usually a complete or near tear. This can be caused by changing directions rapidly, stopping suddenly, slowing down while running, landing from a jump incorrectly, or direct contact or collision. In addition, ACL injuries are related to long-term clinical sequel which includes meniscal tears, chondral lesions, and an increased risk of early onset post-traumatic osteoarthritis [2]. ACL injuries have greatly impacted humans. In humans, ACL injuries are the most common knee injuries [2]. Around 120,000 people suffer from ACL injuries annually in the US [2]. The economic impact of ACL injuries estimating 1.7 billion US dollar [2]. Patients have suffered extensively due to the treatment not being able to give fully access to the use of the ligament.

ACL injury treatment has changed over the years. An early treatment in the early 1900's for ruptured ligaments was using suture. A study was then conducted in the 1970's and showed that over 90% of the patients that received the treatment had failed primary repair. Treatment for humans can be either surgical or non-surgical. For non-surgical treatment, a brace or physical therapy is used. Although non-surgical treatment will not heal a torn ACL, it is effective for patients who are elderly or have a low activity level [5]. Currently, the reconstruction of the ACL consists of removing the ACL and inserting a graft. The graft is either an allograft or an autograft. An allograft is a graft from a cadaver while an autograft is a graft coming from the patient [5]. For the graft, the tissue is taken from tendon such as the medial hamstring or the middle third patellar tendon [2].The actual procedure is done by using an arthroscope with small incisions [5]. Due to the poor regeneration capacity, low cell density, low nutrient requirements, and low oxygen requirements, ACL repairs are prone to re-injury [6]. Issues can arise from the normal reconstruction such as the restoration of normal joint kinematics and kinetics [2, 7].

Furthermore, the issues arise from the insertion, alignment, loss of tissue neurosensory function, graft tissue degeneration, and neuromuscular deficit [2]. Another factor that can affect the surgical treatment is the use of the allograft or autograft. Use of autograft is associated with tissue morbidity while allograft is associated with high risk of biological incorporation failure and disease transmission [2]. Although the current reconstruction is promising, there is still more improvement needed in the treatment procedures.

The analogous structure in canines is the cranial cruciate ligament (CrCL). It is found in the same location as the human ACL and operates in a similar manner. For canines, the major diseases associated with the cranial cruciate ligaments are cranial cruciate ligament disease and cranial cruciate rupture. Cranial cruciate ligament rupture causes hind limb lameness in canines and is commonly misdiagnosed [8]. Small breed dogs develop ruptures from long standing patella luxation or acute trauma while large breed dogs develop ruptures from two main causes. The first is an acute CrCL from strenuous activity. It can occur from hyperextension and/or excessive strain. The second cause, is from slow degeneration of the ligament. Some risk factors include, obesity, neutering, degeneration associated with aging, excessively straight hind limb, immune mediated arthropathies, increased tibia plateau, and excessive patellar ligament plateau angle [8]. Alike ACL injuries, CrCL injuries have also greatly. As seen, there are many risk factors involved with the disease and is common amongst dogs. The disease itself accounted for 1.32 billion dollars in 2003 [8]. Moreover, the disease has doubled over the past 30 years [8]. It is important that there be a way to combat this disease by either preventative care, improved diagnostic procedures, or treatment strategies. The difference between dogs and humans is that the main cause for dogs is associated with aging while human’s injury occurs mainly from

impact. In addition, the injuries in dogs is seen from radiographs and can be observed over time [8].

1.2. Tissue Engineering

ACL reconstruction is traditionally performed using autologous tendinous tissue or allogenic ACL. Both are associated with donor site morbidity, longer surgery time, and paucity of cadaveric ACL. Tissue engineering is a field of study aiming to create de novo tissue to replace the need for current autologous or allogenic implants. To create successful implantable de novo tissue, 3 components play a vital role in tissue engineering, scaffolds as void filler and base for cellular attachment, cells, and defined culture environment such as growth factors [3, 9]. Common materials for tissue engineering are synthetic polymers, metals, and biologic material such as algae, collagen, and silk. Ceramics that are used for tissue engineering are hydroxyapatite and tri-calcium phosphate. Ceramics are typically used for bone regeneration due to their brittleness and high mechanical stiffness. Synthetic polymers that are used for scaffolds are polystyrene, poly-l-lactic acid (PLLA), polyglycolic acid (PGA), and poly-dl-lactic-co-glycolic acid (PLGA). A commonly known natural polymer is collagen. These materials are fabricated to prepare scaffolds by multiple modalities including electrospinning, mold creation, crochet, and 3D-printing. Successful scaffolds require biocompatibility, biodegradability, mechanical properties [3]. Biocompatibility is the acceptance of a non-natural implant by surrounding tissue and the body, and biocompatible materials allow cells must adhere, function normally, and migrate to the surface. The main types of inflammatory cells that interact with biomaterials are macrophages and giant cells [10]. Biodegradability is critical, as non-degradable materials may elicit chronic inflammatory response. Upon implantation minimal inflammatory response that can be resolved and not elicit cytotoxicity degrade materials overtime [11].

Mechanical properties of materials play important role, as scaffold has to withstand force applied to during manipulation under surgery and after implantation until replaced by native tissue. And material used to fabricate scaffolds is main contributor of mechanical properties. Additionally, architecture of the scaffold contributes to mechanical properties, such as porosity of scaffolds. Porosity is important not only for mechanical properties but also interconnected pore structure allows larger space for cells to distribute, adequate exchange of nutrient and oxygen with waste [3]. A large pore size and porosity is important for permeability but could risk mechanical strength [12]. Ultimately, tissue engineering would create a simpler surgical technique, decrease patient morbidity, decrease risk for infection, decrease disease transmission, improved fixation methods, and provide a rapid return of function to the ligament.

1.3. Materials

As materials to fabricate scaffold, PLA, PGA, polydioxanone (PDS), and collagen are appealing as they are commercially available and their properties are well characterized. PLA is an aliphatic polymer and possess amorphous properties. It is a degradable polymer which takes between 10 months to 4 years to fully degrade. The time it takes to degrade is dependent on molecular weight, crystallinity, shape, and implantation site. It degrades into lactic acid by desertification. Mechanically, PLA had an ultimate tensile load of 175 N in a braided structure [3]. PGA is a rigid thermoplastic and is not soluble in most organic solvents. The properties and degradation of PGA is ultimately determined by the processing techniques. PGA degrades to glycolic acid by two stages of the diffusion of water into the amorphous regions of the matrix and simple hydraulic chain scission of the ester group of the molecule, followed by crystalline areas erosion [13]. PDS is largely used as suture material. It is a biodegradable polymer which is derived from the monomer paradioxanone. The material itself is flexible and high strength

retention. It also has a slow absorption rate. The material also has low surface friction which allows for the material to glide through tissue. A disadvantage to this material is the inability to maintain shape memory. PDS can also be electro spun to create scaffolds with a certain porosity, surface area, and surface volume [14]. Collagen itself accounts for 80% of the molecular weight of ligaments. Within ligaments, collagen is cross-linked which provides strength for the ligament. As compared to the PLA braided scaffold, the collagen scaffolds are sown to have lower tensile loads and ultimate strengths. However, collagen is more biodegradable than the synthetic polymers. Advantage of collagen is superior biodegradability and biocompatibility. Collagen is degraded by catabolic processes [3].

1.4. Stem Cells

Stem cells are unspecialized cells which are capable of differentiating to other cells. The different types of stem cells are embryonic stem cells, fetal stem cells, and adult stem cells. Embryonic stem cells can be collected from internal cellular mass of blastocyst [15]. They are called pluripotent that can develop into cells all lineages in the ectoderm, endoderm, and mesoderm [15]. The fetal stem cells are accumulated in the liver of the fetus. Fetal stem cells can be considered multipotent due to the 200 different cell types it can differentiate into [16]. Fetal stem cells and embryonic stem cells can be implanted if they are less than 12 weeks old [15]. Adult stem cells can be harvested from any tissue of adult individual throughout body including blood, cornea, bone marrow, dental pulp, brain, skeletal muscle, skin, liver, pancreas, and gastrointestinal tract [17]. They are more specialized and usually have differential potential towards lineages of origin. Mesenchymal stem cells are one of the most commonly used adult stem cells due to ease of collection, lack of ethical concerns, and negligible risk of teratoma formation[18]. Specifically, adipose stem cells are used due to their abundance and method of

collecting [19]. The cells which are used for ligament regeneration are mesenchymal stem cells due to their differentiation potential. Mesenchymal stem cells can generate into connective tissue such as blood, muscle, bone, etc. [15].

2. Materials and Methods

2.1. Scaffold Designs for 3D Printing

Scaffolds to fabricate by conventional- or bio-3D printer were designed using Fusion 360 (Autodesk, Inc., San Rafael, CA) Triangle truss-like pattern was rendered to sheet of 16.77 mm x 2.5 mm x 60 mm which was rolled to oval tube of 10 mm x 7 mm x 62 mm to approximate the size of CrCL from middle size dogs (Fig. 1B). Oval tube was then rotated to 30° about longitudinal axis to mimic native CrCL morphology (Fig. 1A & Fig. 2). Mold (Fig. 1D & Fig. 5) and tray (Fig. 6) were also designed to fabricate triangle pattern sheet using lyophization of biomaterial, such as collagen.

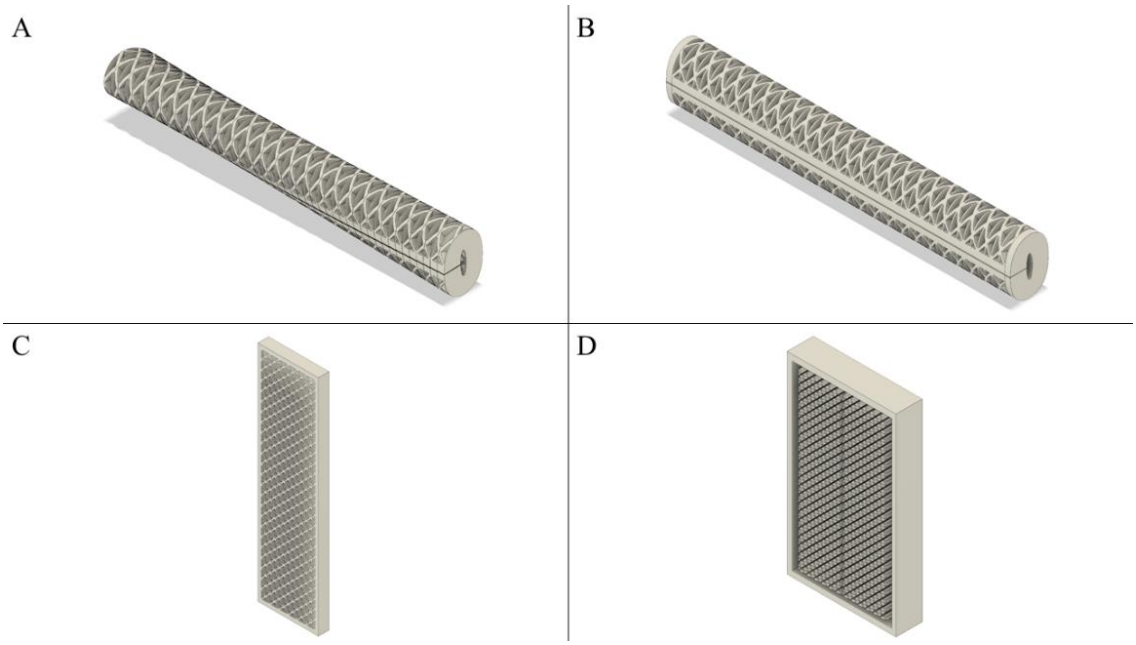

Figure 1. Design of oval tube scaffold and mold/tray design. (A) Oval tube scaffold rotated 30° about longitudinal axis (B) Oval tube scaffold (C) Sheet design (D) Mold to fabricate triangle pattern sheet.

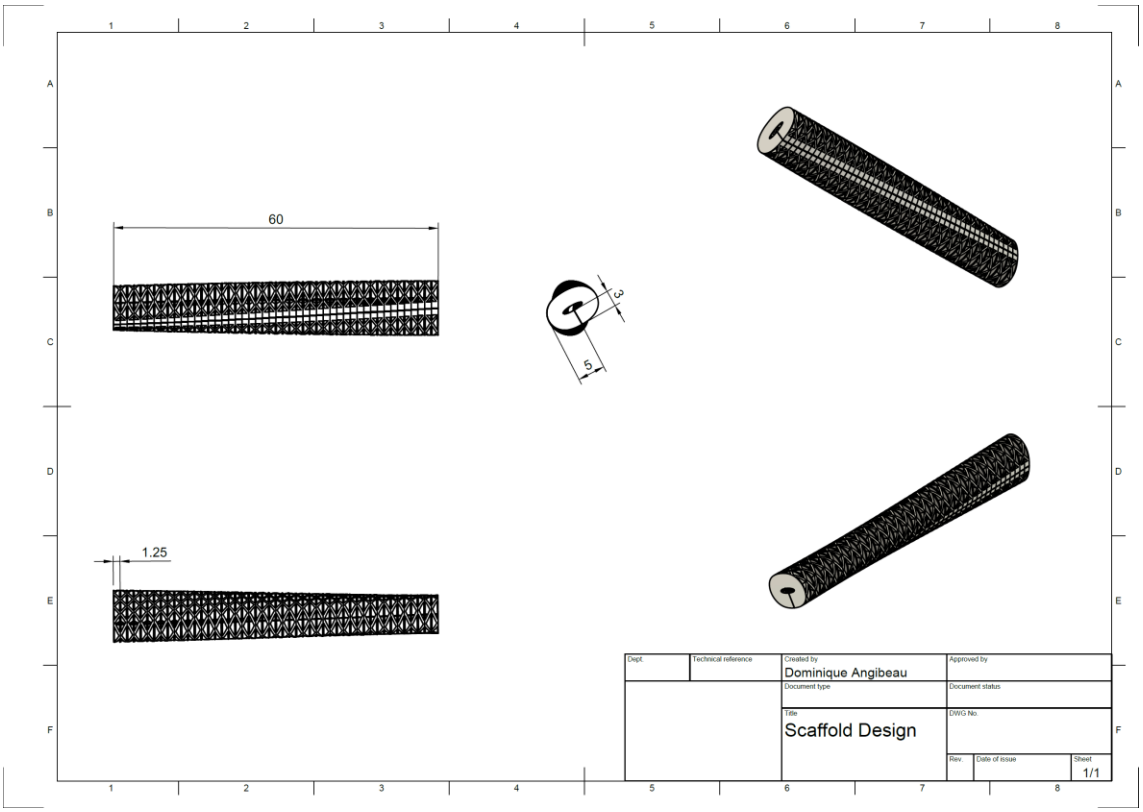

Figure 2. The oval design twisted at 30° is displayed in drawing format. The height of the scaffold is 60 mm with a major diameter of 5 mm and a minor diameter of 3 mm. Each row of the triangular patter is 1.25 mm tall.

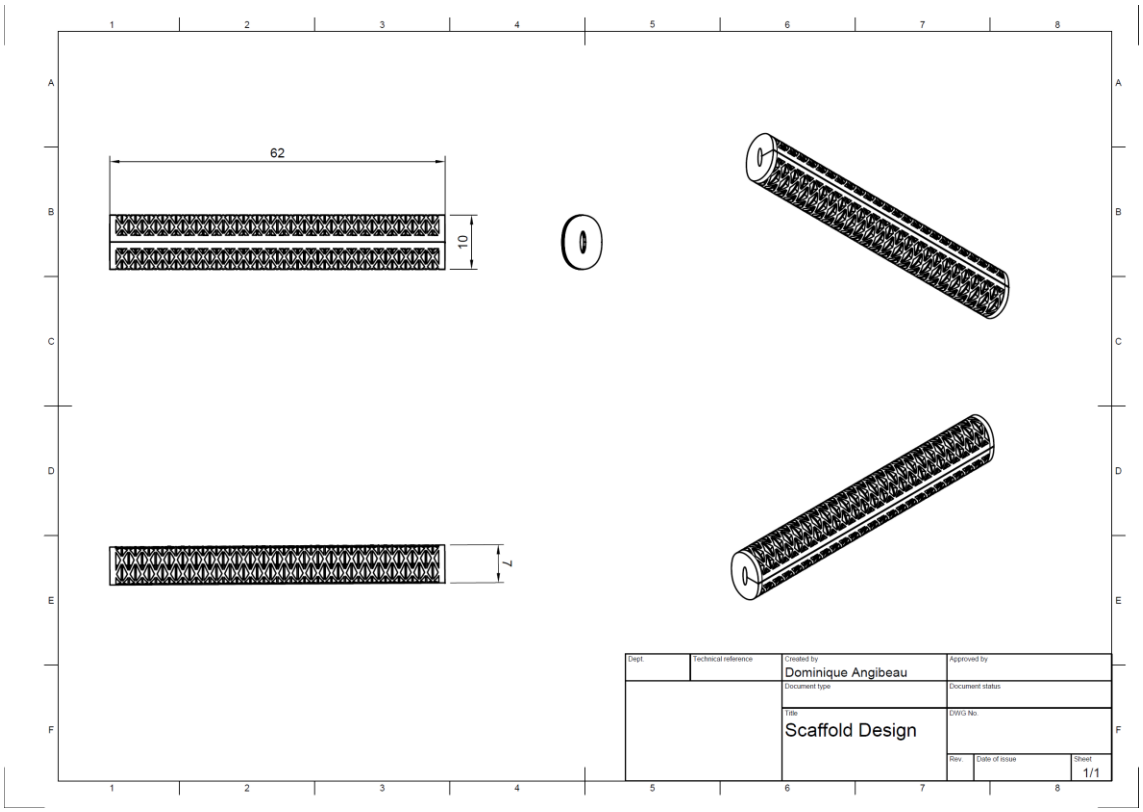

Figure 3. Oval tube design drawing. The major diameter is 10 mm and the minor diameter is 6 mm. The length of the scaffold if 62 mm.

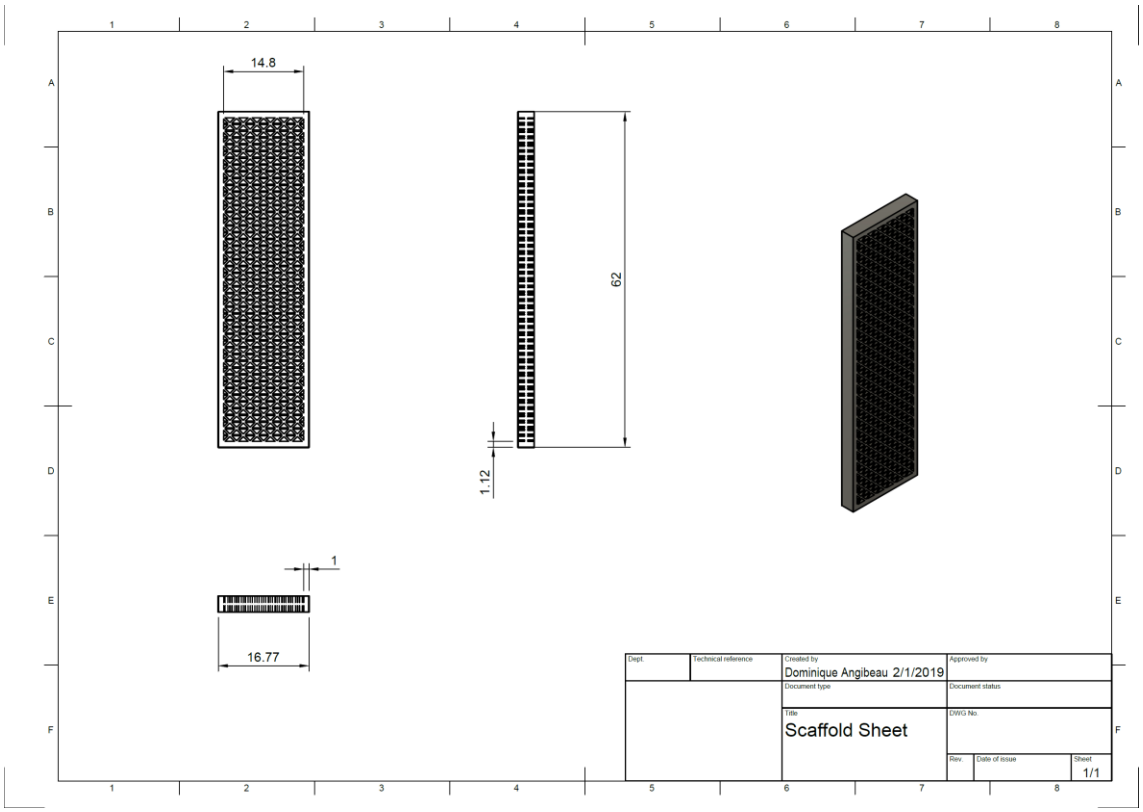

Figure 4. Scaffold sheet design drawing. The sheet has a height of 62 mm and width of 16.77 mm. The pattern itself is 14.8 mm wide and 59.76 mm tall. The thickness on the sides is 1 mm while the thickness on the top and bottom is 1.12 mm.

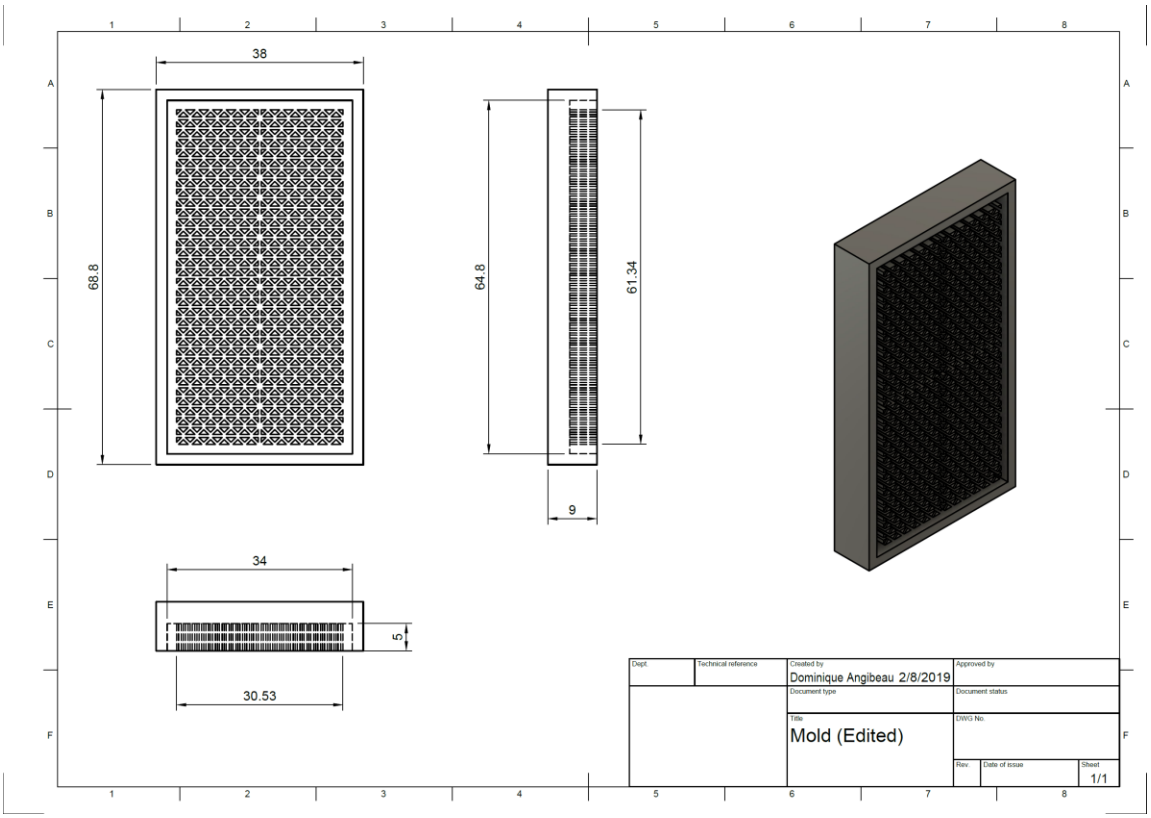

Figure 5. Scaffold mold design drawing. The total height is 68.8 mm and 38 mm wide. The entire mold is 9 mm thick. The portion where it will mold the design is 34 mm wide, 64.8 mm tall, and 5 mm deep.

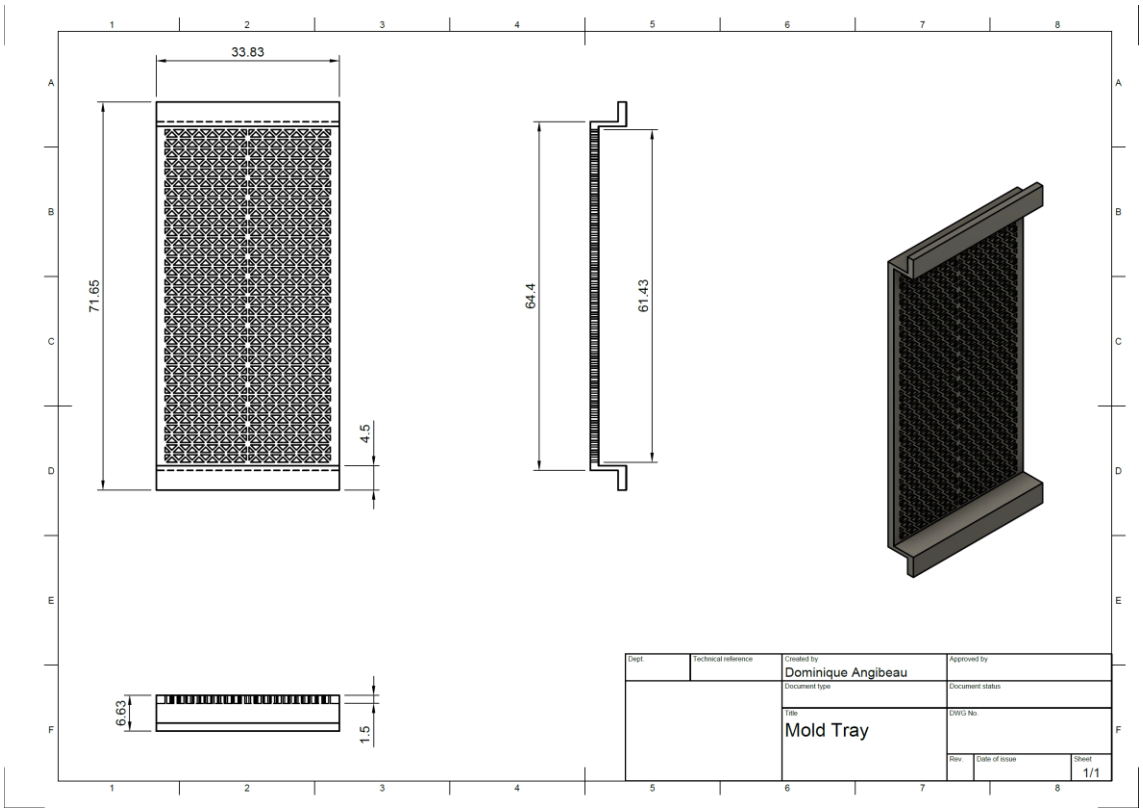

Figure 6. Tray design drawing. The tray is 71.65 mm tall and 33.83 mm wide. It is 1.5 m thick and a depth of 5.13. The tray is designed to fit into the mold design.

2.2. Static Stress Simulation

Prior to printing, static stress simulation was performed to select best material for scaffold fabrication. The materials tested were PGA, PLLA, and PDS. Properties of these materials were obtained from MatWeb and other sources [13, 20-26]. The materials were inserted into the materials index of Fusion 360. A 400 N of tensile force was applied on both ends of scaffold design. The parameters observed included safety factors, displacement, stress, reaction force, and strain [27].

The safety factor is a ratio of the yield stress and the working stress. It determines the safety of the material and its failure. If the number is greater than 1, then the material and structure is safe to use for a particular strength.

$$Safety\ Factor = \frac{Yield\ Strength}{Working\ Strength}$$

The displacement, of the scaffold if determined by the amount it is moved from its original place.

$$\delta = \Delta L$$

The von Mises strength is a part of the strength which relates to the failure of a structure. Within von misses, there are principle stresses. Von Mises is the theory that a structure will yield if the von Mises strength is greater than or equal to the yield strength

$$\sigma' \geq S_y$$

$$\sigma' = \left[\frac{(\sigma_1 - \sigma_2)^2 + (\sigma_2 - \sigma_3)^2 + (\sigma_3 - \sigma_1)^2}{2}\right]^{1/2}$$

The strain, is a ratio of the change in length over the initial length. The strain can be taken from all angles. In particular, the stress analysis simulation observed shows the total strain.

$$\varepsilon = \frac{\delta}{L}$$

The stiffness of a structure is the applied force over the deflection. It is the resistance to the deflection by an applied force to an elastic body.

$$k = \frac{F}{\delta}$$

2.3. Fabrication of Scaffolds

To establish culture system for ligament constructs, 2 types of scaffolds were prepare with biocompatible collagen and PDS suture (Fig. 3). Briefly, eight-figure loop of PDS suture (Fig. 3A) was wrapped by lyophilized bovine collagen type I (COLI) sponge (Fig. 3B, Avetene®, BARD, Warwick, RI) secured by PDS suture with Chinese finger trap pattern (Fig. 3C). To render triangle pattern to COLI sponge, PDS suture was sawn horizontally (Fig. 3D).

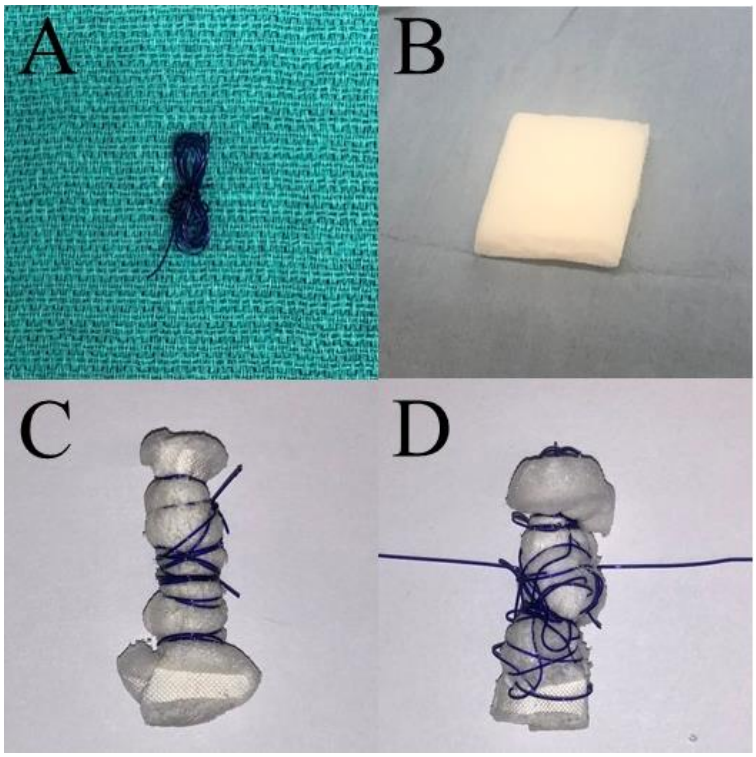

Figure 7. COLI scaffold preparation using PDS suture and COLI sponge. PDS suture is looped around into eight-figure structure (A) and then wrapped around by COLI sponge (B), secured by PDS suture using Chinese finger trap pattern (C). To render triangle pattern of designed scaffold, PDS suture was sawn horizontally to COLI sponge, followed by identical preparation procedure as scaffold shown in C (D).

2.4. Construct Preparation and Incubation

Canine infrapatellar adipose tissue-derived multipotent stromal cells (cIFP-ASC) were isolated from infrapatellar fat pad of 6 adult mix-breed dogs by 0.1% type I collagenase digestion at 37°C. cIFP-ASCs were cultured in stromal medium (DMEM-Ham's F12 supplemented with 10% FBS and 1% antibiotic/antimitotic) shown in figure 7. COLI scaffolds were incubated with bovine fibronectin (10 µg/ml) for 30 min and secured in custom-designed bioreactor (Fig. 4A, B). Bioreactor housing COLI was connected to perfusion culture system consisted of gas-exchange chamber and PC-controlled pneumatic pump (Fig. 4C) and cultured with cIFP-ASCs in stromal medium (Fig. 4D) for 7 days.

Figure 8**.** Perfusion bioreactor system to culture ligament construct. Each end of the COLI scaffold was tied to horizontal bars in the cylinder housing construct to maintain tension (A, B). Cylinder was connected to gas-exchange chamber (bottom part) and peristaltic pump (not

shown) with tube (C). COLI scaffold was loaded with cIFP-ASCs and incubated in perfusion bioreactor system maintained in 5% CO2 and 37°C (D).

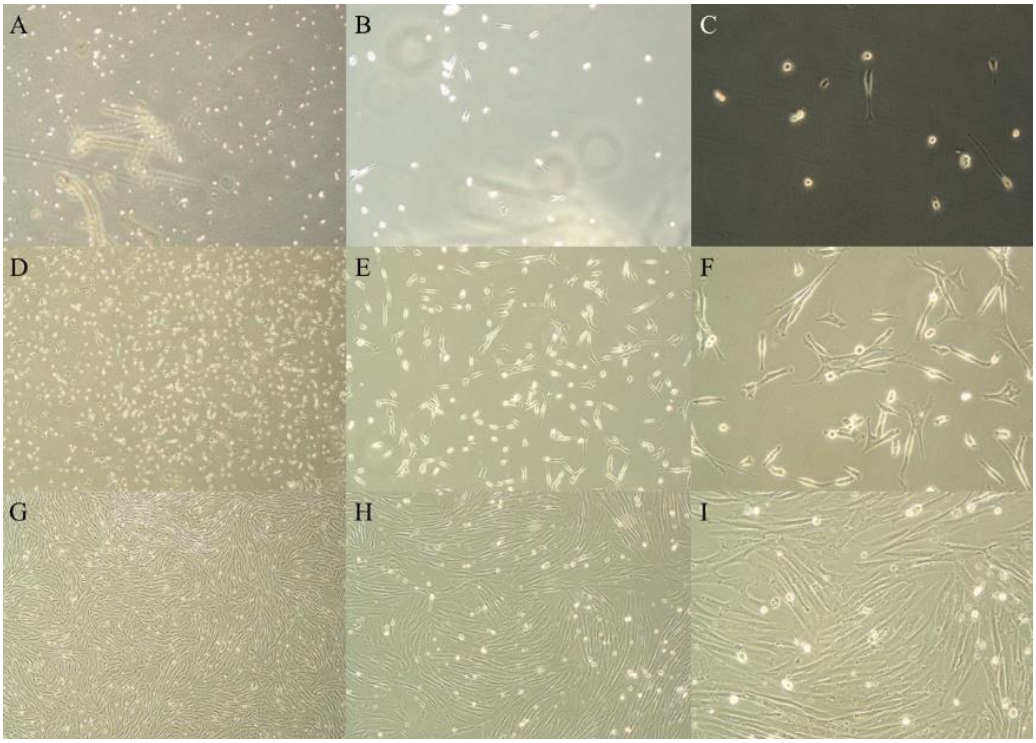

Figure 9. Morphology of cIFP-ASCs observed by inverted bright field microscope. cIFP-ASCs with approximately 20% confluency at day 1 (A – C), with 50% confluency at day 4 (D – F), and with 100% confluency at day 7 (G – I). Magnification 4X (A, D and G), 10X (B, E and H) and 20X (C, F and I)

3. Results

3.1. 3D Printing of Scaffold

The oval tube scaffold and mold/tray designs were printable by stereolithography at the resolution of 0.4572 mm. Figure 10 displays the oval tube structure. The smallest entity on the scaffold is 0.508 mm. The mold/tray design is displayed in figure 11. The smallest entity is 0.4572 mm.

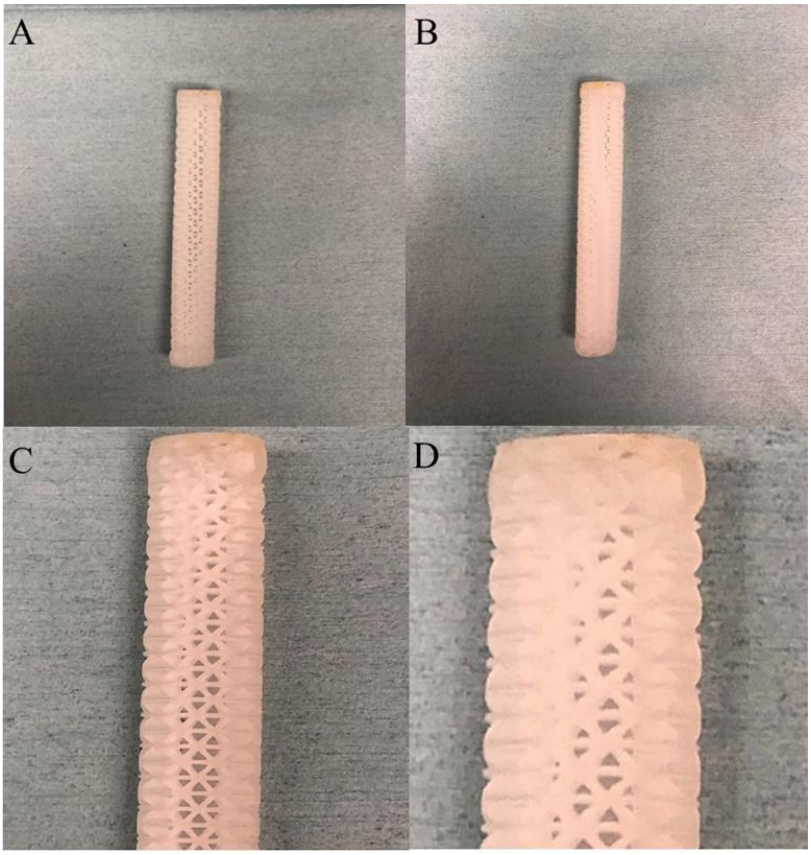

Figure 10. Oval tube scaffold rotated 30° about longitudinal axis printed by stereolithography. Gross appearance of scaffold from both side of oval long axis (A and B). Close up partial views of scaffold to illustrate triangle truss-like pattern in scaffold (C and D).

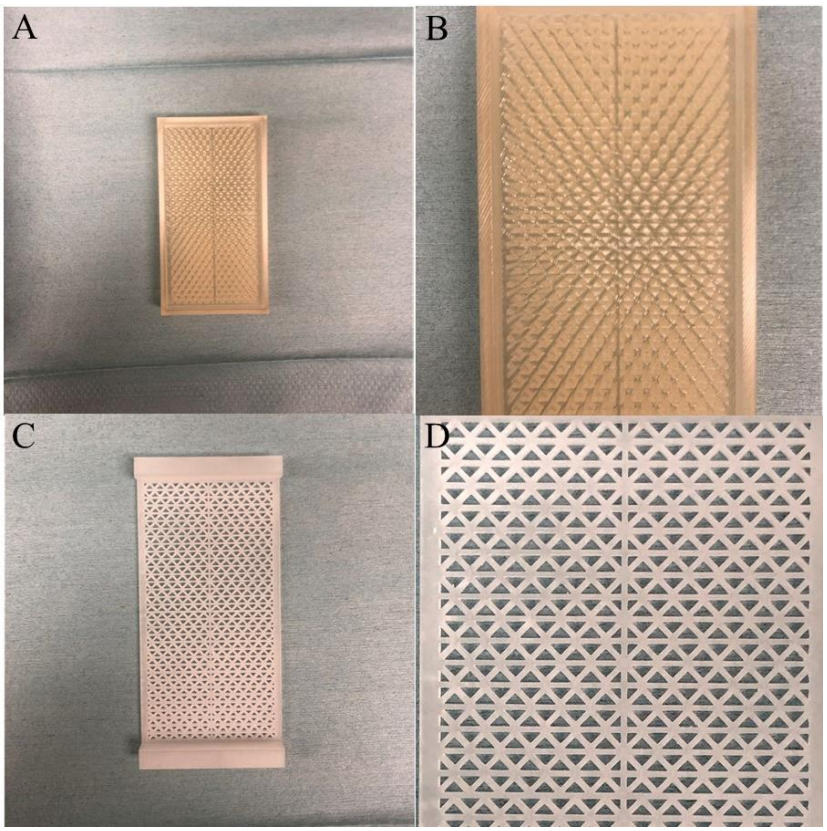

Figure 11. Mold and tray to fabricate triangle pattern sheet printed by stereolithography. Gross appearance (A) and close up partial view (B) of the mold with groove of triangle truss-like pattern. Gross (C) and close up partial view (D) of tray with strut of triangle truss-like pattern, which fits in groove of mold. Tray functions to lift lyophilized sheet.

3.2. Static Stress Simulation

The synthetic polymers all had a safety factor of 15 while collagen has a safety factor of 0.01818. Between the synthetic polymers, PGA had the highest minimum safety factor. Collagen exhibited the highest minimum displacement. As shown in figure 13, largest displacement in collagen scaffold centered on the edges. For the other 3 synthetic polymers, PGA exhibits the lowest minimum displacement, at 0.007353 mm, following PDS, with 0.01926 mm, and PLA with 0.647 mm. The lowest maximum displacement is also PGA with 0.3056 mm. Looking at

strain, the behavior is similar to that of displacement, with collagen having the highest minimum and maximum strain, along with PGA having the lowest. The stiffness was calculated by using the stiffness equation, applied force, and displacements calculated from the static stress analysis. PGA, exhibited the highest stiffness at 54399.56 N/mm. The two other synthetic polymers, PDS and PLA, exhibited a max stiffness of 20768.43 N/mm and 618.238 N/mm. Figure 16 displays the stiffness and failure load of a human ACL and CrCL. Although they were calculated in slightly different ways, they still give an insight on how the ligament reacts. The stiffness of PGA and PDS will be able to sustain the stiffness of the human ACL and CrCL. The minimum stiffness of PGA and PDS were, 1308.901 N/mm and 525.0722 N/mm. Both of these materials should be able to sustain the stiffness of a human ACL and CrCL.

It is quite apparent that PGA is mechanically stronger material, but from the information about PGA, it is not as biocompatible, biodegradable, and prosperous with cell growth, as PDS, PLA, and collagen. Collagen obviously exhibits weakness mechanically. Although there were difference in the results with the four materials, the places in which the impact occurred on the scaffold was similar.

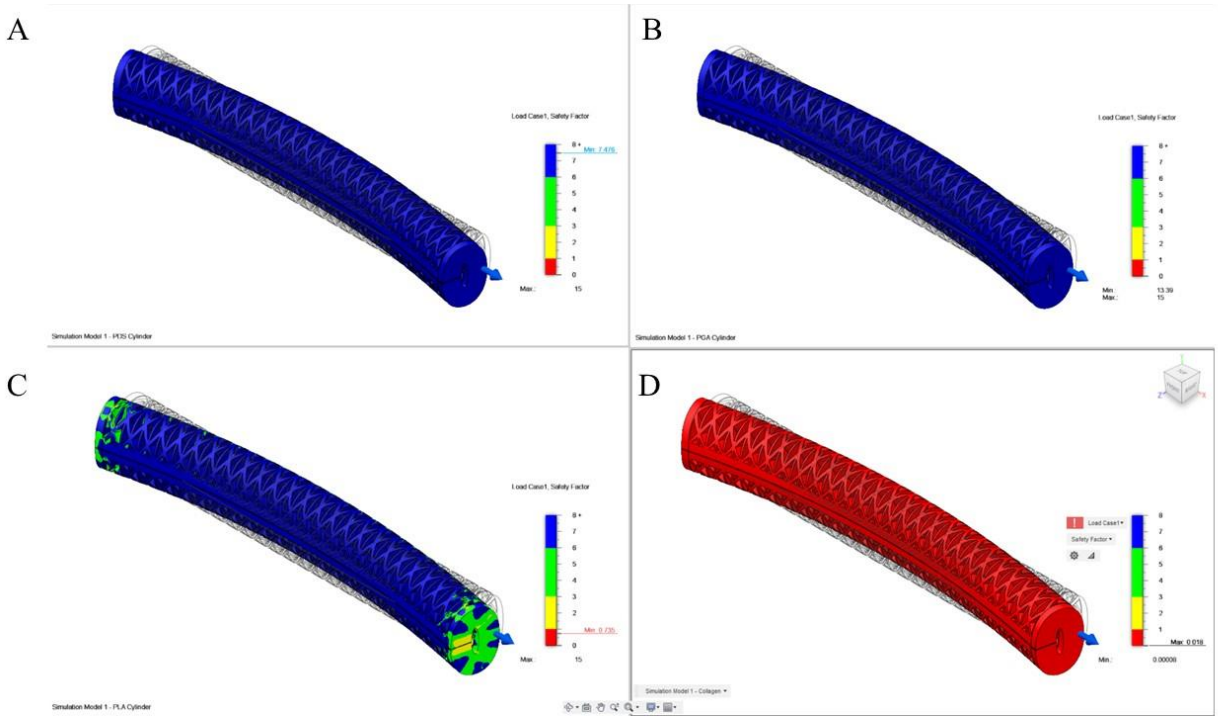

Figure 12. Safety factor results. Colors in the scale represent lower value toward red and higher value toward dark blue. PDS (A), PGA (B), PLA (C), and Collagen (D) are shown.

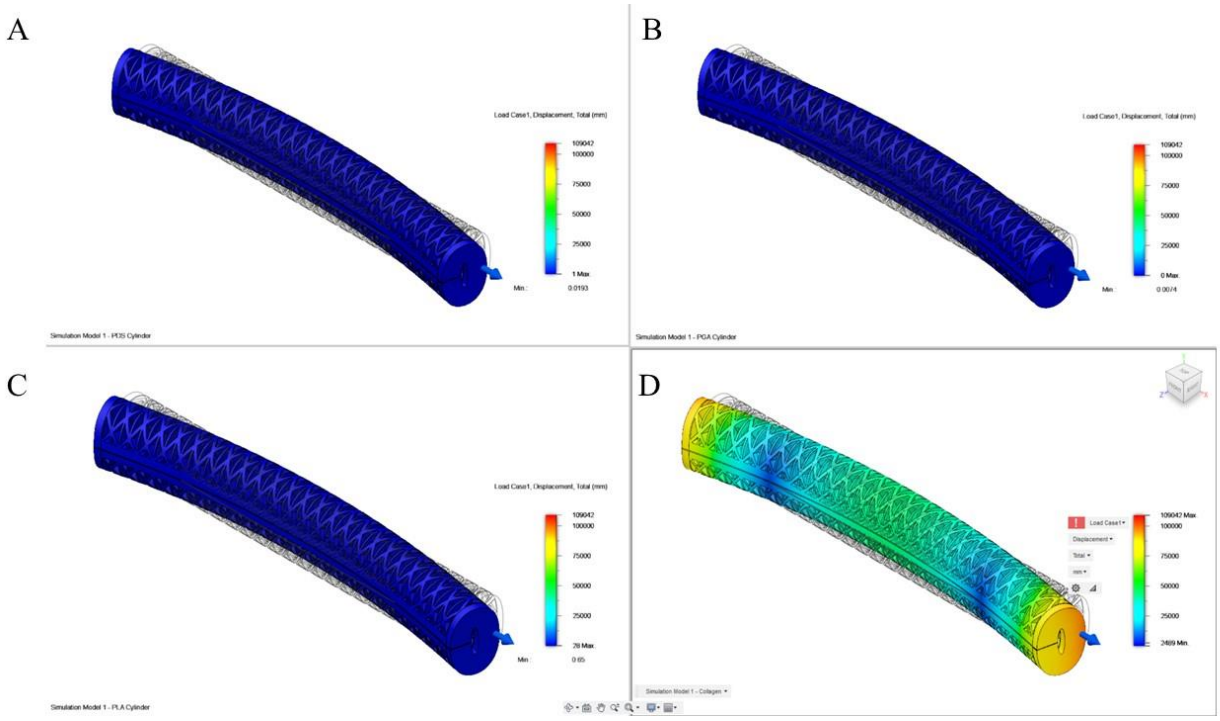

Figure 13. Displacement results. Colors in the scale represent lower value toward dark blue and higher value toward red. PDS (A), PGA (B), PLA (C), and Collagen (D) are shown.

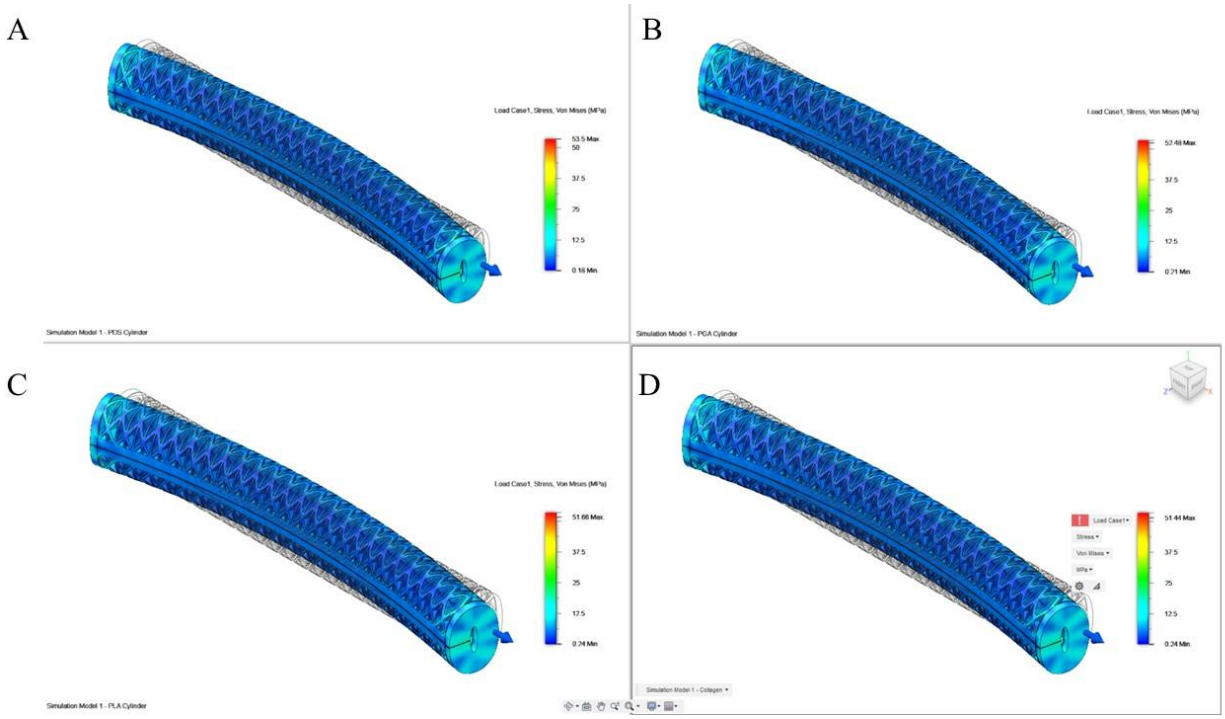

Figure 14. Von Mises results. Colors in the scale represent lower value toward dark blue and higher value toward red. PDS (A), PGA (B), PLA (C), and Collagen (D) are shown.

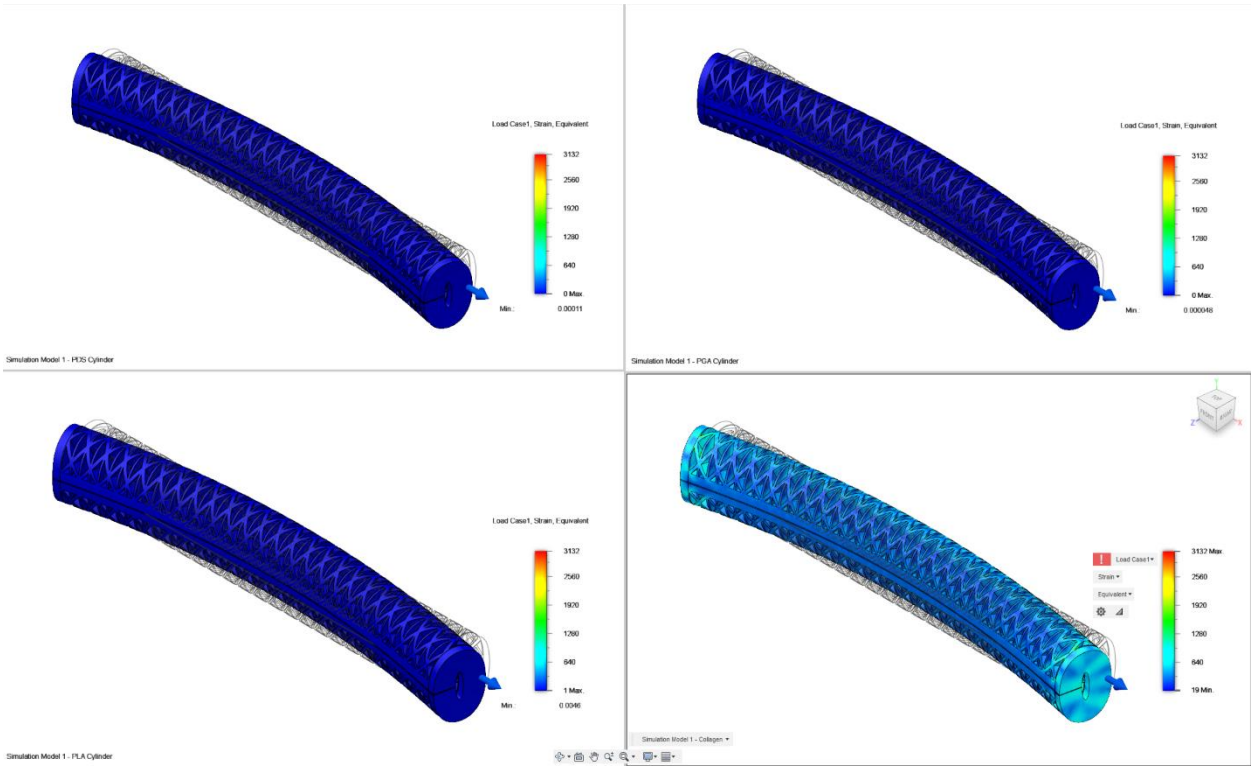

Figure 15. Strain results. Colors in the scale represent lower value toward red and higher value toward dark blue. PDS (A), PGA (B), PLA (C), and Collagen (D) are shown.

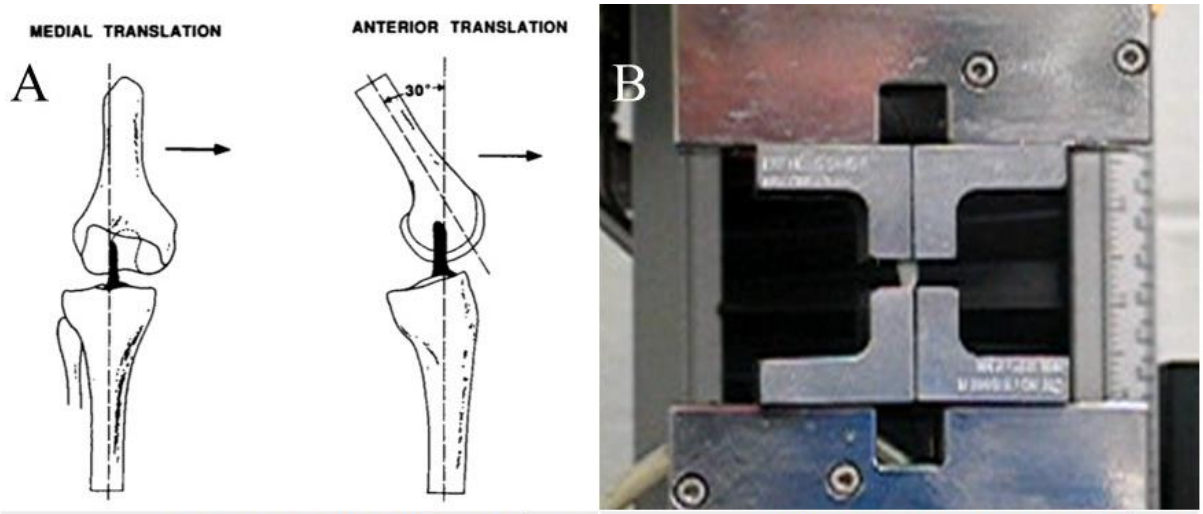

	Failure Load (N)	Stiffness (N/mm)
Human ACL	1602 ± 167	218 ± 27

	Failure Load (N)	Stiffness (N/mm)
CrCL	243.8 ± 7.4	117.4 ± 21.3

Figure 16. Failure load and stiffness of a human ACL and canine CrCL as a reference for simulation. Mechanical properties of human ACL was conducted by a tensile test in a tibial orientation (A) [27]. Mechanical properties of native CrCL was obtained by unilateral tensile test with original gap of 5 mm and displacement rate of 1 cm/min.

Table 1. The table contains the minimum and maximum results of the static stress analysis.

	Safety Factor		Von Mises (MPa)		Displacement (mm)		Strain		Stiffness (N/mm)	
Material	**Min.**	**Max.**	**Min.**	**Max.**	**Min.**	**Max.**	**Min.**	**Max.**	**Min.**	**Max.**
PDS	7.476	15	0.177	53.5	0.01926	0.7618	1.10E-04	0.02457	525.0722	20768.43
PGA	13.39	15	0.2072	52.48	0.007353	0.3056	4.84E-05	0.00936	1308.901	54399.56
PLA	0.7346	15	0.2444	51.66	0.647	28.02	0.00464	0.8171	14.27552	618.238
Collagen	7.95E-05	0.01818	0.2382	51.44	2489	109042	18.6	3132	0.003668	0.160707

4. Discussion

Mechanically, PGA was superior to other materials for scaffold fabrication. However, PGA has been shown to be less biocompatible and biodegradable. Compared to synthetic polymers,

collagen's mechanical strength was almost negligible, although this biomaterial is known to surpass synthetic polymers in terms of biocompatibility and biodegradability. Regardless of scaffold materials, force applied was concentrated on each end of scaffold. To withstand the stress concentrated on each end, denser structure may be needed on each end along with a thicker mesh structure. Based on static stress simulation, oval tube scaffold fabricated by PGA and PDS far exceeded mechanical properties of native ACL and CrCL. To achieve mechanical strength and biocompatibility, PGA/collagen combined material is suggested as suitable material for scaffold fabrication.

Different scaffolds have been created with using different materials and different configurations. For example, the de novo scaffold using the COLI sponge and PDS suture. The scaffold was able to sustain a substantial amount of mechanical strength but not as much as the 3D designed scaffold. Other scaffold designs include collagen sponge, electrospinning, and braiding. The collagen sponges exhibited a cellular growth but was lacking in mechanical strength. The 3D designed scaffold is different from previously made scaffolds due to its design and configuration. In previously made scaffolds, the designs are made by hand. By using Fusion360, a custom made scaffold was created in order to exhibit the mechanical properties needed for ACL reconstruction. The pattern of the scaffold itself, is a major difference from other scaffolds.

In order to have optimum cells growth and mechanical properties, more material research should be conducted. Furthermore, studies concerning bioprinting should be conducted in order to effectively 3D print scaffold designs. As for the design itself, cell proliferation and cell growth should be tested with the design along with materials. In addition, instron testing should be conducted to see the actual mechanical properties of the scaffolds. A next step would be

observing fixation methods. Since this is a ligament, there is a transition from soft tissue to bone. Studies have been conducted to inquire fixation methods for ACL reconstruction. Lastly, errors in printing should be observed. The printed scaffolds should be measured and compared to that of the 3D software in order to see where there are errors in printing.

5. Conclusion

For future studies, hybrid biomaterials should be tested in order to see the implications of this pattern. The implications of materials is success of scaffolds and with a material that is partially natural and partially synthetic, will allow for optimum strength and muscle growth. In regards to design, the pattern can be altered by making the pores smaller to increase the strength or by trying a diamond pattern rather than a triangle.

ACL and CrCL injuries are the most common knee injuries seen in humans and canines. The impact of a tissue engineering can greatly change the reconstruction for these injuries. Furthermore, the use of tissue engineering and this design, can greatly change the lives of many. In addition, the use of 3D design software and 3D printing can be used to generate custom made entities for patients so that their treatment is unique to their needs.

Bibliography

1. Majewski, M., H. Susanne, and S. Klaus, *Epidemiology of athletic knee injuries: A 10-year study.* Knee, 2006. **13**(3): p. 184-8.
2. Kiapour, A.M. and M.M. Murray, *Basic science of anterior cruciate ligament injury and repair.* Bone & joint research, 2014. **3**(2): p. 20-31.
3. Ge, Z., et al., *Biomaterials and scaffolds for ligament tissue engineering.* Journal of Biomedical Materials Research Part A, 2006. **77A**(3): p. 639-652.
4. Murray, M., P. Vavken, and B. Fleming, *The ACL Handbook: Knee Biology, Mechanics, and Treatment*. 2013.
5. *Anterior Cruciate Ligament (ACL) Injuries*. Disease & Conditions 2014 May 2014 [cited 2014 May 2014].
6. Molloy, T., Y. Wang, and G. Murrell, *The roles of growth factors in tendon and ligament healing.* Sports Med, 2003. **33**(5): p. 381-94.
7. Hall, M., C.A. Stevermer, and J.C. Gillette, *Gait analysis post anterior cruciate ligament reconstruction: knee osteoarthritis perspective.* Gait Posture, 2012. **36**(1): p. 56-60.
8. Roush, J.K., *Canine Cranial Cruciate Disease: Updating Our Knowledge about Pathogenesis & Diagnosis*, in *Today's Veterinary Practice*. 2013, North American Veterinary Community
9. O'Brien, F.J., *Biomaterials & scaffolds for tissue engineering.* Materials Today, 2011. **14**(3): p. 88-95.
10. Williams, D.F., *On the mechanisms of biocompatibility.* Biomaterials, 2008. **29**(20): p. 2941-2953.

11. Rezwan, K., et al., *Biodegradable and bioactive porous polymer/inorganic composite scaffolds for bone tissue engineering.* Biomaterials, 2006. **27**(18): p. 3413-3431.

12. Wu, S., et al., *Biomimetic porous scaffolds for bone tissue engineering.* Materials Science and Engineering: R: Reports, 2014. **80**: p. 1-36.

13. Montes de Oca, H. and I.M. Ward, *Structure and mechanical properties of PGA crystals and fibres.* Polymer, 2006. **47**(20): p. 7070-7077.

14. Boland, E.D., et al., *Electrospinning polydioxanone for biomedical applications.* Acta Biomaterialia, 2005. **1**(1): p. 115-123.

15. Pavlovic, M. and B. Balint, *Stem Cells and Tissue Engineering*. 2012.

16. Tran, J., T.J. Brenner, and S. DiNardo, *Somatic control over the germline stem cell lineage during Drosophila spermatogenesis.* Nature, 2000. **407**(6805): p. 754-7.

17. Balint, B., et al., *Stem cells in the arrangement of bone marrow repopulation and regenerative medicine.* Vojnosanit Pregl, 2007. **64**(7): p. 481-4.

18. Wei, X., et al., *Mesenchymal stem cells: a new trend for cell therapy.* Acta pharmacologica Sinica, 2013. **34**(6): p. 747-754.

19. Bajek, A., et al., *Adipose-Derived Stem Cells as a Tool in Cell-Based Therapies.* Archivum immunologiae et therapiae experimentalis, 2016. **64**(6): p. 443-454.

20. Farah, S., D.G. Anderson, and R. Langer, *Physical and mechanical properties of PLA, and their functions in widespread applications — A comprehensive review.* Advanced Drug Delivery Reviews, 2016. **107**: p. 367-392.

21. Wells, H.C., et al., *Poisson's ratio of collagen fibrils measured by small angle X-ray scattering of strained bovine pericardium.* Journal of Applied Physics, 2015. **117**(4): p. 044701.

22. Yang, L., et al., *Mechanical properties of native and cross-linked type I collagen fibrils.* Biophys J, 2008. **94**(6): p. 2204-11.

23. Beldjilali-Labro, M., et al., *Biomaterials in Tendon and Skeletal Muscle Tissue Engineering: Current Trends and Challenges.* Materials, 2018. **11**(7): p. 1116.

24. Daniels, A.U., M. Lui, and K. Andriano, *Mechanical properties of biodegradable polymers and composites for internal fixation of bone*. Vol. 1. 1990. 57-78.

25. Greenwald, D., et al., *Mechanical comparison of 10 suture materials before and after in vivo incubation.* J Surg Res, 1994. **56**(4): p. 372-7.

26. Kreszinger, M., et al., *Tensile strength retention of resorptive suture materials applied in the stomach wall - An in vitro study*. Vol. 88. 2018. 235-243.

27. Woo, S.L.-Y., et al., *Tensile properties of the human femur-anterior cruciate ligament-tibia complex:The effects of specimen age and orientation.* The American Journal of Sports Medicine, 1991. **19**(3): p. 217-225.